

Submitted to ApJL February 8th; Accepted March 13th

Waves and Instabilities in Accretion Disks: MHD Spectroscopic Analysis

R. Keppens, F. Casse, and J.P. Goedbloed

*FOM Institute for Plasma Physics Rijnhuizen,
P.O. Box 1207, 3430 BE Nieuwegein, The Netherlands
keppens@rijnh.nl, fcasse@rijnh.nl, goedbloed@rijnh.nl*

ABSTRACT

A complete analytical and numerical treatment of all magnetohydrodynamic waves and instabilities for radially stratified, magnetized accretion disks is presented. The instabilities are a possible source of anomalous transport. While recovering results on known hydrodynamic and both weak- and strong-field magnetohydrodynamic perturbations, the full magnetohydrodynamic spectra for a realistic accretion disk model demonstrates a much richer variety of instabilities accessible to the plasma than previously realized. We show that both weakly and strongly magnetized accretion disks are prone to strong non-axisymmetric instabilities. The ability to characterize all waves arising in accretion disks holds great promise for magnetohydrodynamic spectroscopic analysis.

Subject headings: Accretion, accretion disks — MHD — instabilities — waves

1. Hydromagnetic stability for stationary equilibria

Magnetohydrodynamic (MHD) spectroscopy (Goedbloed et al. 1994) entails the ability to calculate all MHD perturbations accessible to a particular magnetized plasma configuration (the *forward* spectral problem), and holds the promise to use the MHD spectrum to diagnose the internal plasma state (the *backward* spectral problem). In this letter, we predict all MHD waves and instabilities for magnetized accretion disks.

To analyse the entire MHD spectrum of gravitationally and thermally stratified, rotating, magnetized equilibrium configurations, we use the formalism of Frieman and Rotenberg (1960). The equation of motion for the Lagrangian displacement $\boldsymbol{\xi}$ of a fluid element is

$$\rho \frac{\partial^2 \boldsymbol{\xi}}{\partial t^2} + 2\rho \mathbf{v} \cdot \nabla \frac{\partial \boldsymbol{\xi}}{\partial t} + \nabla \Pi - \mathbf{B} \cdot \nabla \mathbf{Q} - \mathbf{Q} \cdot \nabla \mathbf{B} + \nabla \cdot (\rho \boldsymbol{\xi}) \mathbf{g} - \nabla \cdot [\rho \boldsymbol{\xi} (\mathbf{v} \cdot \nabla) \mathbf{v} - \rho \mathbf{v} \mathbf{v} \cdot \nabla \boldsymbol{\xi}] = 0, \quad (1)$$

where $\Pi = -\boldsymbol{\xi} \cdot \nabla p - \gamma p \nabla \cdot \boldsymbol{\xi} + \mathbf{B} \cdot \mathbf{Q}$ measures the Eulerian perturbation of total pressure, $\mathbf{Q} = \nabla \times (\boldsymbol{\xi} \times \mathbf{B})$ is the Eulerian perturbation of the magnetic field \mathbf{B} , and \mathbf{g} is the gravitational acceleration. Equation (1) describes all waves supported by a time-invariant equilibrium with density ρ , pressure p , flow field \mathbf{v} , gravity \mathbf{g} , and \mathbf{B} ; γ is the ratio of specific heats. We specify our analysis to one-dimensional (1D) axisymmetric stationary equilibria satisfying

$$\left(p + \frac{B_\theta^2 + B_z^2}{2} \right)' = \rho \left(\frac{v_\theta^2}{r} - \frac{G_c M_*}{r^2} \right) - \frac{B_\theta^2}{r}, \quad (2)$$

where the prime denotes differentiation with respect to the radial coordinate r from a (r, θ, z) cylindrical system. Hence, we concentrate on wave motions about an equilibrium where centrifugal forces, gravity, pressure gradients and magnetic forces balance. The one-dimensionality limits the generality by representing the gravitational influence of a central body of mass M_* by a line source $\mathbf{g}(r) = -G_c M_*/r^2 \hat{\mathbf{e}}_r$, but this at most introduces a vertical wavelength cut-off on the validity of our results.

The equilibrium symmetry allows for a decoupled analysis of individual normal mode solutions where $\boldsymbol{\xi}(r, \theta, z, t) = (\xi_r(r), \xi_\theta(r), \xi_z(r)) \exp i(m\theta + kz - \omega t)$. For the radially varying magnetized equilibria, it is instructive to use a field line projection which introduces the basic variables $\hat{\chi} = r\xi_r$, $\hat{\eta} = ir(\mathbf{B}/B \times \hat{\mathbf{e}}_r) \cdot \boldsymbol{\xi}$ and $\hat{\zeta} = ir\mathbf{B}/B \cdot \boldsymbol{\xi}$. It is then a matter of algebra to turn the Frieman-Rosenbluth system (1) into

$$\begin{aligned} & \left[\begin{array}{ccc} \left(r D_r \frac{\gamma p + B^2}{r} D_r - F^2 - r \left(\frac{B_\theta^2}{r^2} \right)' & r D_r \frac{\gamma p + B^2}{r} \frac{G}{B} - 2k \frac{B_\theta B}{r} & r D_r \frac{\gamma p}{r} \frac{F}{B} \\ -\frac{G}{B} (\gamma p + B^2) D_r - 2k \frac{B_\theta B}{r} & -(\gamma p + B^2) \frac{G^2}{B^2} - F^2 & -\gamma p \frac{GF}{B^2} \\ -\gamma p \frac{F}{B} D_r & -\gamma p \frac{GF}{B^2} & -\gamma p \frac{F^2}{B^2} \end{array} \right] \\ & + \begin{pmatrix} \frac{3G_c M_*}{r^3} \rho & -\rho V_g \frac{G}{B} & -\rho V_g \frac{F}{B} \\ -\rho V_g \frac{G}{B} & 0 & 0 \\ -\rho V_g \frac{F}{B} & 0 & 0 \end{pmatrix} + 2\rho \frac{v_\theta}{r} \tilde{\omega} \begin{pmatrix} 0 & -\frac{B_z}{B} & -\frac{B_\theta}{B} \\ -\frac{B_z}{B} & 0 & 0 \\ -\frac{B_\theta}{B} & 0 & 0 \end{pmatrix} + \rho \tilde{\omega}^2 \mathbf{I} \begin{pmatrix} \hat{\chi} \\ \hat{\eta} \\ \hat{\zeta} \end{pmatrix} = 0 \quad (3) \end{aligned}$$

In this system, the radial derivative operator is denoted by D_r , while the parallel gradient operator becomes the algebraic factor $F \equiv -i\mathbf{B} \cdot \nabla = mB_\theta/r + kB_z$. Furthermore, $G \equiv mB_z/r - kB_\theta$ and $V_g \equiv v_\theta^2/r - G_c M_*/r^2$. The latter measures the deviation from a Keplerian disk. The terms linearly proportional to the Doppler shifted frequency $\tilde{\omega} = \omega - mv_\theta/r - kv_z$ represent the Coriolis effect. For static cylindrical equilibria without external gravitational field, this representation of the eigenvalue problem was introduced in Goedbloed (1975).

From Equation (3), one can immediately obtain the Alfvén and slow continuous parts of the ideal MHD spectrum by looking at extreme localization of the perturbations on single flux surfaces ($D_r \rightarrow \infty$). The first component can then be integrated at once, and, when inserted in the second and third, yields $A\hat{\eta} = 0$ and $S\hat{\zeta} = 0$, respectively. The Alfvén continuum

corresponds to singular solutions $\hat{\eta} \propto \delta(r - r_A)$, where $A(r_A) \equiv (\rho\tilde{\omega}^2 - F^2)(r_A) = 0$. The slow modes are given by $\hat{\zeta} \propto \delta(r - r_S)$, where $S(r_S) \equiv (\rho\tilde{\omega}^2(\gamma p + B^2) - \gamma p F^2)(r_S) = 0$. Due to the radial variation of the equilibrium and the Doppler shift, four continuous ranges of real eigenfrequencies are found. With the cluster points $\tilde{\omega} = \pm\infty$ for the fast subspectrum, these Doppler shifted forward and backward Alfvén and slow continua determine the three-fold structure of the MHD spectrum. These continua are not influenced by gravity or rotation.

An interesting limit of this system has obtained a lot of attention in the accretion disk literature. Considering a weakly magnetized accretion disk, it is possible to show that the combination of differential rotation with a weak magnetic field introduces a linear ‘weak-field shearing’ MHD instability (Balbus and Hawley 1991). As recently discussed in the review by Balbus and Hawley (1998), one can derive a sixth order dispersion relation governing local linear disturbances with purely vertical wave numbers $\mathbf{k} = k\hat{\mathbf{e}}_z$ in disks where the restricted hydrodynamic equilibrium relation $V_g = 0$ holds. This dispersion relation for axisymmetric $m = 0$ modes is formally found from Equation (3) by setting $D_r = 0$, neglecting all curvature terms where B_θ appears explicitly, and by using $V_g = 0$. It can then be written as

$$\begin{aligned} & \left(\tilde{\omega}^2 - \frac{F^2}{\rho} \right) \left(\tilde{\omega}^4 - k^2 \tilde{\omega}^2 \left(c_s^2 + \frac{B^2}{\rho} \right) + \frac{F^2}{\rho} k^2 c_s^2 \right) \\ & - \left[\kappa^2 \tilde{\omega}^4 - \tilde{\omega}^2 \left(k^2 \kappa^2 \left(c_s^2 + \frac{B_\theta^2}{\rho} \right) - 3 \frac{G_c M_* F^2}{r^3 \rho} \right) \right] + 3 \frac{G_c M_* F^2}{r^3 \rho} k^2 c_s^2 = 0. \end{aligned} \quad (4)$$

Here, $\kappa^2 \equiv 2v_\theta(rv_\theta)'/r^2 = G_c M_*/r^3$ is the epicyclic frequency and the squared sound speed is $c_s^2 = \gamma p/\rho$. This equation suggests marginal stability for $F^2/\rho = 3G_c M_*/r^3$.

An equivalent formulation of the MHD eigenvalue problem for equilibria satisfying (2) reduces the Frieman-Rosenbluth system to a 2×2 system in terms of the variables $(\hat{\chi}, \Pi)$:

$$\frac{AS}{r} \begin{pmatrix} \hat{\chi} \\ \Pi \end{pmatrix}' + \begin{pmatrix} C & D \\ E & -C \end{pmatrix} \begin{pmatrix} \hat{\chi} \\ \Pi \end{pmatrix} = 0. \quad (5)$$

In this equation, the following terms appear

$$C = \frac{\rho}{r} V_g \rho \tilde{\omega}^2 A + \frac{2m}{r^3} (B_\theta F + \rho v_\theta \tilde{\omega}) S - 2 \frac{\rho^2 \tilde{\omega}^3 B_\theta}{r^2} (B_\theta \tilde{\omega} + v_\theta F), \quad (6)$$

$$D = \rho^2 \tilde{\omega}^4 - \left(\frac{m^2}{r^2} + k^2 \right) S, \quad (7)$$

$$\begin{aligned} E = & \frac{AS}{r} \left[-\frac{A}{r} - \left(\frac{B_\theta^2}{r^2} \right)' + \frac{\rho}{r} \kappa^2 + \frac{\rho'}{r} V_g - \frac{\rho^2}{r} V_g^2 \frac{A}{S} + 4\rho^2 \tilde{\omega} \frac{B_\theta}{r^2} V_g \frac{B_\theta \tilde{\omega} + v_\theta F}{S} \right] \\ & - \frac{4}{r^4} \left[\rho^2 \tilde{\omega}^2 B_\theta^2 (B_\theta \tilde{\omega} + v_\theta F)^2 - ([B_\theta^2 + \rho v_\theta^2] F + 2\rho \tilde{\omega} v_\theta B_\theta) F S \right]. \end{aligned} \quad (8)$$

This system (5) reduces to the normal mode picture by Appert et al. (1974) for static cylindrical equilibria without gravity. Bondeson et al. (1987) and Hameiri (1976) derived this system for cylindrical equilibria with flow, without gravity. An analysis for gravitating, flowing, magnetized equilibria in planar geometry is found in van der Holst et al. (1999).

The set of equations (5) again demonstrates that the continuous part of the MHD spectrum is found from $A = 0$ and $S = 0$. The ranges in frequency where $D = 0$ are not part of the continuous spectrum: for details, see Goedbloed (1998). Either of the formalisms given by the set (3), system (5), or the equivalent second order Sturm-Liouville type equation can be used to analyse the MHD spectrum of magnetized accretion disks. In particular, assuming a radial variation $\exp(ik_r r)$ we obtain a local dispersion relation given by

$$k_r^2 \frac{A^2 S^2}{r^2} + C^2 + DE = 0. \quad (9)$$

Similar to the static case, or the more general one including flow (Bondeson et al. 1987), one can prove the proportionality $C^2 + DE \propto AS$, so that the continua $AS = 0$ can be factored out. This leaves a sixth order polynomial in $\tilde{\omega}$ which governs all discrete local modes. Again, as a formal limit obtained by nullifying terms where m , k_r , or B_θ appears explicitly, and assuming a Keplerian equilibrium $V_g = 0$, this polynomial is the dispersion relation (4). The more general relation (9) leads immediately to the following marginal stability criterion governing axisymmetric perturbations when $B_\theta = 0$

$$F^2 \left\{ (k_r^2 + k^2) \frac{F^2}{\rho} + k^2 \left(\kappa^2 - \frac{4v_\theta^2}{r^2} - \frac{V_g^2}{c_s^2} + \frac{\rho'}{\rho} V_g \right) \right\} = 0. \quad (10)$$

The multiplicative factor $F^2 = k^2 B_z^2$ highlights the essential magnetic character of this criterion. For non-vanishing B_θ , even the $m = 0$ case of equation (9) allows for overstable or damped MHD waves. The general relation (9) recovers various known results. Terquem and Papaloizou (1996) presented a stability analysis of accretion disks with both radial and vertical equilibrium variations, but a purely toroidal B_θ magnetic field. In particular, a stability criterion for axisymmetric perturbations required a parameter defined in their equation (29) to be positive. If one considers only radial equilibrium variation, the same is found from our dispersion relation (9). Kim and Ostriker (2000) analyzed the stability of a cold ($p = 0$) radially stratified disk. Our relation (2) contains their equilibrium as a special case, and their results form a subset of our analysis. E.g., their equation (43) for ‘poloidal buoyancy modes’ follows from (9) by taking $m = B_\theta = v_z = 0$ and assuming $k_z^2 B_z^2 / \rho \gg \tilde{\omega}^2$. As a final note on the system (5), the pure hydrodynamical limit can be written as

$$\begin{pmatrix} \hat{\chi} \\ \Pi \end{pmatrix}' + \begin{pmatrix} \frac{\rho'}{\gamma p} + 2 \frac{mv_\theta}{r^2 \tilde{\omega}} & r \frac{\tilde{\omega}^2 - \left(\frac{m^2}{r^2} + k^2\right) c_s^2}{\rho c_s^2 \tilde{\omega}^2} \\ \left(\frac{\rho'}{\rho} - \frac{\rho'}{\gamma p}\right) \frac{\rho'}{r} - \frac{\rho}{r} (\tilde{\omega}^2 - \kappa^2) & -\frac{\rho'}{\gamma p} - 2 \frac{mv_\theta}{r^2 \tilde{\omega}} \end{pmatrix} \begin{pmatrix} \hat{\chi} \\ \Pi \end{pmatrix} = 0. \quad (11)$$

The continuous part of the spectrum is now collapsed onto the flow continuum $\tilde{\omega}^2 = 0$ (Case 1960). The local dispersion relation (9) with this flow continuum factored out reads

$$k_r^2 c_s^2 \tilde{\omega}^2 + c_s^2 \left(2 \frac{m v_\theta}{r^2} + \tilde{\omega} \frac{p'}{\gamma p} \right)^2 + \left[\tilde{\omega}^2 - \left(\frac{m^2}{r^2} + k^2 \right) c_s^2 \right] \left[\kappa^2 - \tilde{\omega}^2 + V_g \left(\frac{\rho'}{\rho} - \frac{p'}{\gamma p} \right) \right] = 0. \quad (12)$$

Several known results are immediately recovered from this relation, especially for $m = 0$ modes where it has a simple solution. For a polytropic equilibrium with $v_z = 0$, the limit where $(k_r, k) \rightarrow \infty$ at a finite ratio k_r/k yields $\tilde{\omega}^2 = \kappa^2 k^2 / (k_r^2 + k^2)$, giving a dense range of discrete modes within $-\kappa < \tilde{\omega} < \kappa$. The same limit shows that stability requires $\kappa^2 > 0$, known as the Rayleigh (1916) criterion. The $m \neq 0$ global modes of equation (12) are of the Papaloizou and Pringle (1984) variety. High m non-axisymmetric instabilities can be inferred from (12), which simplifies in the incompressible limit ($\gamma \rightarrow \infty$, $\rho' \rightarrow 0$) to a bi-squared relation. For weakly magnetized disks, the modes contained in the dispersion relation (12) will be complemented by Alfvénic and slow magnetosonic perturbations.

2. Full spectral analysis of accretion disks

With the general formalism for a complete normal mode analysis of magnetized accretion disks in place, we present in the remainder full MHD spectra for a specific thin disk model satisfying (2). We use an analytical model of a disk where the ratio $\beta = 2p/B^2$ is r -independent. Two other parameters are the constant helicity of the magnetic field $\alpha = -B_\theta/B_z$, and the disk aspect ratio $\varepsilon = H/r \ll 1$, where H is the disk scale height. If one neglects radiative pressure in the disk, ε measures the ratio of the sound to the Keplerian speed $\varepsilon = c_s/\Omega_k r$ (Shakura and Sunyaev 1973). Because of the Newtonian gravitational field, we describe the physical quantities using radial power laws. To have a constant ε , c_s must scale as $r^{-1/2}$. The density profile is set to $\rho \propto r^{-3/2}$. For the pressure and magnetic field we use the $r^{-1/2}$ scaling of c_s and the constant β . The inner radius, the density and the Keplerian velocity at the inner radius make all quantities dimensionless. The resulting disk structure is: $\rho = r^{-3/2}$, $p = \varepsilon^2 r^{-5/2}$, magnetic field $B_z = \varepsilon \sqrt{2} r^{-5/4} / \sqrt{\beta(1 + \alpha^2)}$ and $B_\theta = -\alpha B_z$. The rotational velocity will then be $v_\theta = v_o r^{-1/2}$, where $v_o(\alpha, \beta, \varepsilon)$ is found from (2). The v_z component is set to zero. We calculate the collection of eigenfrequencies by a generalization of the LEDAFLOW program (Nijboer et al. 1997). LEDAFLOW computes the entire MHD spectrum of 1D, gravitationally stratified, magnetized equilibria with flow by solving the linearised MHD equations. The radial discretization for the eigenfunctions employs quadratic and cubic Hermite finite elements, appropriate for both global and (near-)singular local modes. We use rigid boundary conditions in the domain $r \in [1, r_{out} = 10]$. We input the parameters for the equilibrium $(\alpha, \beta, \varepsilon)$ and the normal mode numbers (m, k) .

Since we consider thin disks, we set $\varepsilon = 0.1$. The helicity of the \mathbf{B} field is taken $\alpha = 1$.

Weakly magnetized accretion disk. We present two calculations for a weakly magnetized accretion disk. We set the parameter $\beta = 2 \cdot 10^3$. Similar to Balbus and Hawley (1998), we first take a purely vertical wave vector $\mathbf{k} = 2\pi/H\mathbf{e}_z$. The vertical wavelength should not exceed the vertical size of the disk. In Fig. (1), we show the MHD spectrum. We can identify all modes in this plot: the fast-magnetosonic, epicyclic, and (overlapping) Alfvén and slow-magnetosonic continuum modes are all on the real axis. A dense sequence of discrete modes appears on the imaginary axis: the magneto-rotational instability. This sequence is the unstable part of the slow magnetosonic subspectrum. Performing the same calculation for $\beta \rightarrow \infty$ (hydrodynamical case), only the epicyclic and sonic modes remain and no unstable mode is found, confirming its slow magnetosonic nature. We present in Fig. (2) the spectrum for non-axisymmetric perturbations with $m = 10, k = 70$. Note the asymmetry due to the Doppler shift $\mathbf{k} \cdot \mathbf{v} \neq 0$. The identification of the different modes is quite involved since the fast, slow, Alfvén and epicyclic frequency ranges are all overlapping. Various branches of unstable modes can be seen, where only the rightmost branches correspond to their axisymmetric analogues already present in Figure (1). The structure suggests the presence of global modes accumulating towards both the Alfvén and the slow continua. A full MHD spectroscopic analysis, which investigates the mode types from their specific polarization properties, is the subject of future work.

Equipartition accretion disk ($\beta = 1$). We performed several calculations of MHD perturbations supported by disks where the magnetic pressure is of the same order as the thermal one. The results we have obtained are quite clear. If the perturbation is non-axisymmetric, unstable branches appear in the spectra. The growth rate of these instabilities grows for increasing m . For the disk equilibrium discussed above, no axisymmetric unstable modes are found. The spectral structure is shown in Fig. (3) for $m = 10$. Because all the terms in Eq. (5) are of the same order, a purely analytical approach is virtually impossible.

3. Concluding remarks

We applied a general formalism to an astrophysical system where most MHD instabilities are believed to occur: the accretion disk. Our analysis covers both unmagnetized and magnetized disks. Complete MHD spectra were presented for equilibria involving the gravity of a central object, velocities v_θ and v_z , and both thermal pressure and a magnetic field with azimuthal and vertical components. We deduced the relations (9), (10), (12), describing the threshold of several known instabilities for a differentially rotating fluid, including the Papaloizou-Pringle modes and the weak-field magneto-rotational one. The relations apply

to fully compressible, non-Keplerian magnetized disks. If one ignores vertical stratification, they generalize the analysis of Papaloizou and Szuszkiewicz (1992), who considered only $m = 0$ modes when no azimuthal B_θ field was present. We complemented our analytical approach with numerical calculations of MHD spectra of a realistic magnetized disk model. MHD spectra for weakly magnetized accretion disks contain the magneto-rotational instability and several other branches of discrete unstable modes. We numerically found a variety of toroidal unstable modes which can affect equipartition accretion disks. Our results are consistent with Noguchi et al. (2000) who made an analysis of non-axisymmetric incompressible modes in accretion disks, and found Alfvénic instabilities for strong magnetic fields. We generalize their findings by considering all MHD modes. Instabilities at equipartition field strengths are of big interest since it is believed that magnetized disks launching MHD jets have a thermal pressure of the same order as the magnetic one (Ferreira and Pelletier 1995). Coppi and Coppi (1998, 2001) have pointed out the importance of anomalous transport produced by non-singular, non-axisymmetric bending modes for the regime of large magnetic energy density. These modes are amongst the instabilities analysed here. A complete MHD spectroscopic study for these and other (also 2D) accretion disk equilibria will be presented in future work (Goedbloed et al. 2002). Since the MHD spectrum for disks which are weakly magnetized or at equipartition field strengths shows this enormous variety of unstable modes, the description of MHD turbulence in magnetized accretion disks is far from complete. Follow-up nonlinear simulations should reveal the importance of the various modes for triggering and sustaining MHD turbulence. The analytical framework presented can be of interest for physical mechanisms involving disk instabilities, such as the ‘Accretion-Ejection Instability’ (Tagger and Pellat 1999) and the hydrodynamical Rossby vortices (Tagger 2001). The study of instabilities affecting radially stratified MHD jets (Kersalé et al. 2000; Appl et al. 2000; Kim and Ostriker 2000) is embedded in the present formalism.

This work was done under Euratom-FOM Association Agreement with financial support from NWO, Euratom, and the European Community’s Human Potential Programme under contract HPRN-CT-2000-00153, PLATON, also acknowledged by F.C.

REFERENCES

- Appert, K., Gruber, R., and Vaclavik, J. 1974, *Phys. Fluids*, 18, 1258.
- Appl, S., Lery T., and Baty, H. 2000, *A&A*, 355, 818
- Balbus, S.A., and Hawley, J.F. 1998, *Rev. Mod. Phys.*, 70, 1

- Balbus, S.A., and Hawley, J.F. 1991, *ApJ*, 376, 214.
- Bondeson, A., Iacono, R., and Bhattacharjee, A. 1987, *Phys. Fluids*, 30, 2167.
- Case, K.M. 1960, *Phys. Fluids*, 3, 143 and 149.
- Coppi, B., and Coppi, P.S. 1998, *Phys. Lett. A*, 239, 261
- Coppi, B., and Coppi, P.S. 2001, *Phys. Rev. Lett.*, 87, 051101
- Ferreira, J., and Pelletier, G. 1995, *A&A*, 295, 807
- Frieman, E., and Rotenberg, M. 1960, *Rev. Mod. Phys.*, 32, 898
- Goedbloed, J.P., Beliën, A.J.C., and van der Holst, B. 2002, *Phys. Rev. Lett.*, submitted.
- Goedbloed, J.P., Poedts, S., Huysmans, G.T.A., Halberstadt, G., Holties, H., and Beliën, A.J.C. 1994, *Fut. Gen. Comp. Systems*, 10, 339
- Goedbloed, J.P. 1975, *Phys. Fluids*, 18, 1258.
- Goedbloed, J.P. 1998, *Phys. Plasmas*, 5, 3143.
- Hameiri, E. 1976, PhD Thesis, New York University.
- van der Holst, B., Nijboer, R.J., and Goedbloed, J.P. 1999, *J. Plasma Phys.*, 61, 221.
- Kersalé, E., Longaretti, P.-Y., and Pelletier, G. 2000, *A&A*, 363, 1166
- Kim, W.T., and Ostriker, E.C. 2000, *ApJ*, 540, 372
- Nijboer, R.J., van der Holst, B., Poedts, S., and Goedbloed, J.P. 1997, *Comp. Phys. Comm.*, 101, 39.
- Nogushi, K., Tajima, T., and Matsumoto, M. 2000, *ApJ*, 541, 802
- Papaloizou, J.C.B., and Pringle, J.E. 1984, *MNRAS*, 208, 721.
- Papaloizou, J.C.B., and Szuszkiewicz, E. 1992, *Geophys. Astrophys. Fluids Dyn.*, 66, 223
- Lord Rayleigh 1916, *Proc. Roy. Soc. A*, 93, 143.
- Shakura, N.I., and Sunyaev, R.A. 1973, *A&A*, 24, 337
- Tagger, M., and Pellat, R. 1999 *A&A*, 349, 1003
- Tagger M., 2001 *A&A*, 380, 750

Terquem, C., and Papaloizou, J.C.B. 1996, MNRAS, 279, 784

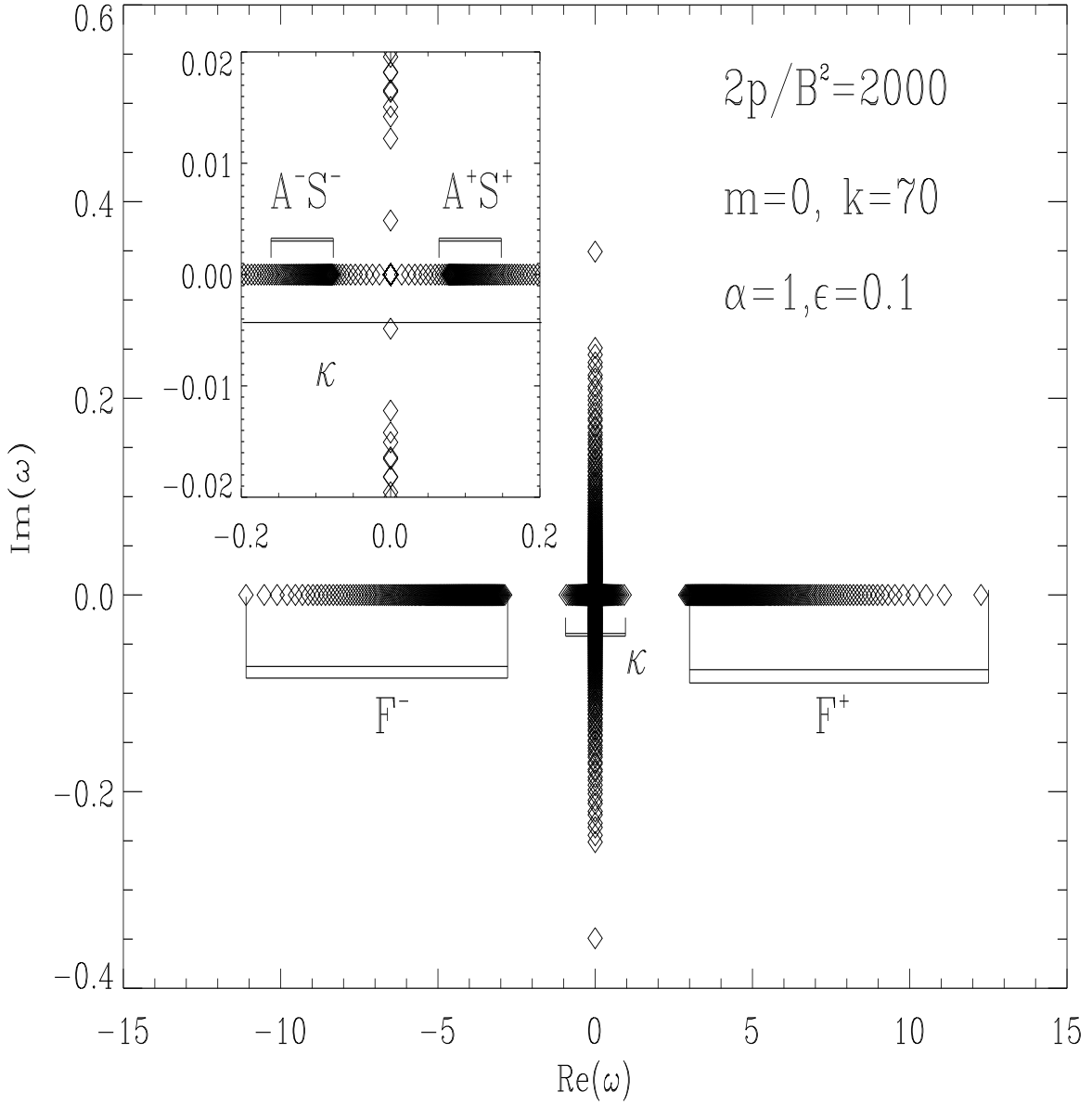


Fig. 1.— MHD spectrum for a weakly magnetized accretion disk for perturbations where $\mathbf{k} = k\mathbf{e}_z$. As the Doppler shift vanishes ($\mathbf{k} \cdot \mathbf{v} = 0$), the identification of the different subspectra is easy (A^\pm, S^\pm for forward and backward Alfvén and Slow modes, κ for the epicyclic ones, and F^\pm for forward and backward fast modes.). The magneto-rotational instability is identified as a cluster spectrum of discrete modes associated with the slow continuum.

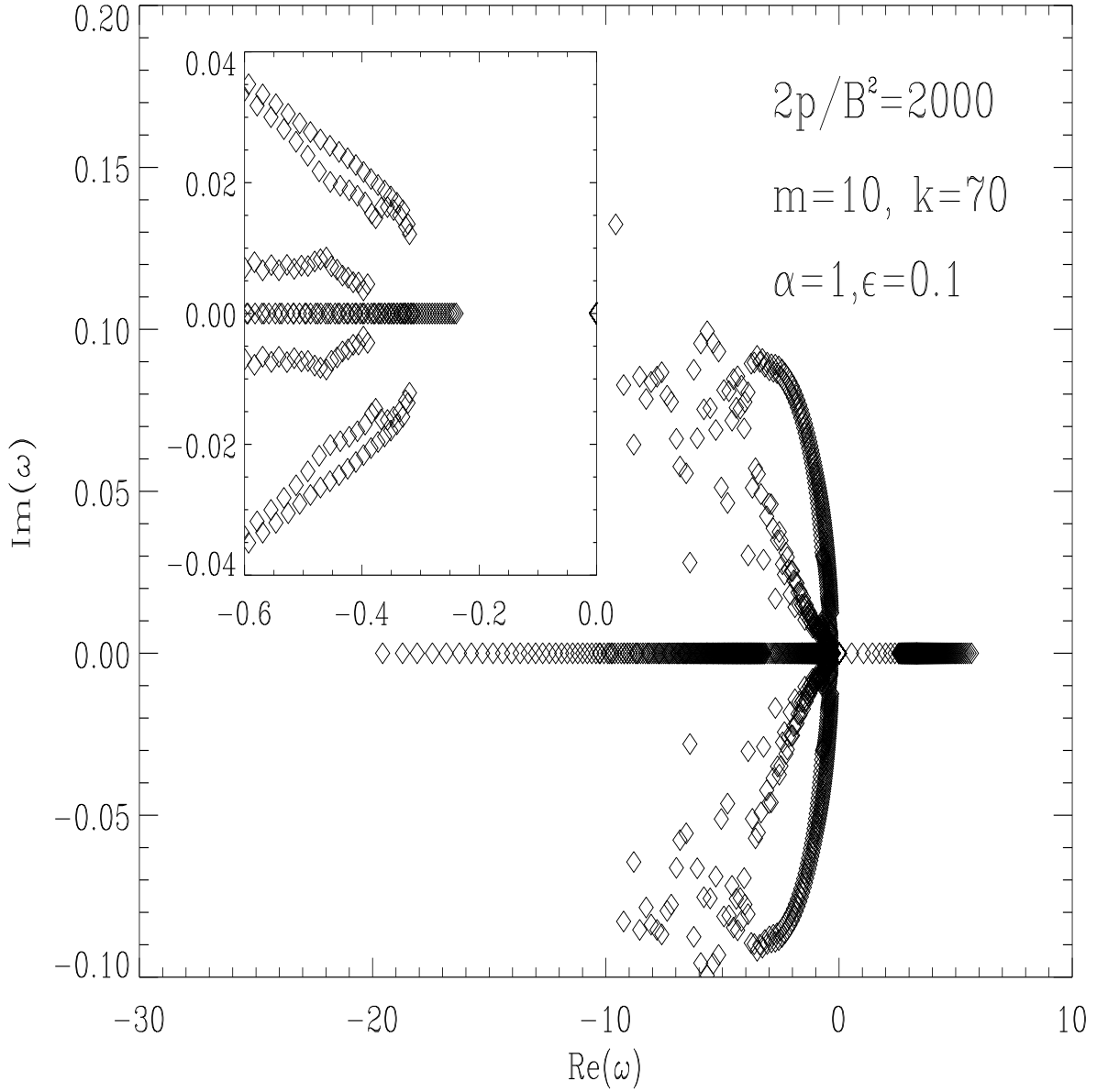


Fig. 2.— As Fig. (1), but for non-axisymmetric perturbations ($m = 10$). All the slow and Alfvénic sub-spectra overlap partially and several cluster branches of unstable modes are apparent.

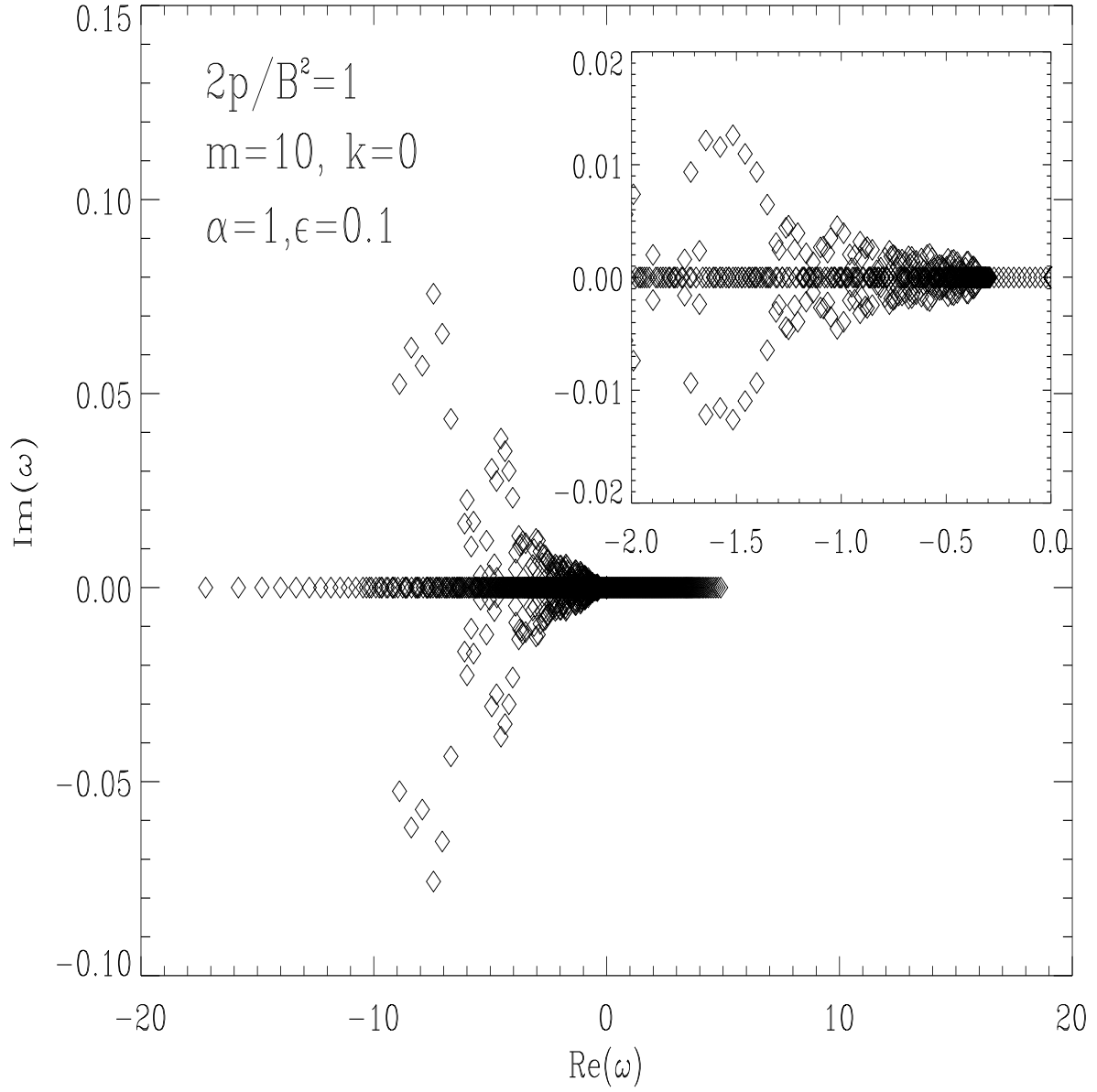


Fig. 3.— MHD spectrum of toroidal perturbations in an equipartition accretion disk ($\beta = 1$). The calculation demonstrates a large collection of unstable modes.